Charles University in Prague
Faculty of Mathematics and Physics

BACHELOR THESIS

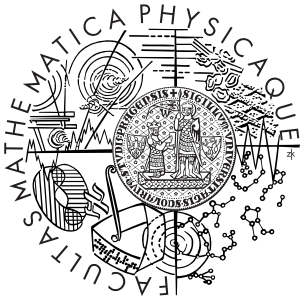

Vlastimil Kůs

Higgs boson production in diffraction processes at LHC

Institute of Particle and Nuclear Physics

Supervisor: RNDr. Alice Valkárová, DrSc.

Study programme: General Physics

2007

First I would like to thank my supervisor, RNDr. Alice Valkárová DrSc., for her help, patience and guidance. My next thanks belongs to Mgr. Marek Taševský Ph.D. for useful discussion. Last but not least, I would like to thank to my family for their support during my whole studies.

I declare that I wrote my bachelor thesis independently and exclusively with the use of the cited sources. I agree with lending and publishing the thesis.

Prohlašuji, že jsem svou bakalářskou práci napsal samostatně a výhradně s použitím citovaných pramenů. Souhlasím se zapůjčováním práce a jejím zveřejňováním.

In Prague, 3rd July 2007 Vlastimil Kůs

Contents

Title: Higgs boson production in diffraction processes at LHC
Author: Vlastimil Kůs
Department: Institute of Particle and Nuclear Physics
Supervisor: RNDr. Alice Valkárová, DrSc.
Supervisor's e-mail address: alice.valkarova@mff.cuni.cz

Abstract: In the present work the Standard Model Higgs' boson production in central exclusive diffractive processes is studied. Our attention is focused to the WW decay mode. The main part of this thesis is in simulations of proton interactions at the LHC collider at CERN for different Higgs' boson masses by the use of the ExHuME Monte Carlo program. Gained data were subsequently processed and analyzed by the ROOT data analysing system. We have found that although a number of events of our interest will be small, a detectable signal for Higgs' masses above 140 GeV can be expected.

Keywords: diffraction, Higgs' boson, ExHuMe program

Název práce: Produkce Higgsova bosonu v difrakčních procesech na LHC
Autor: Vlastimil Kůs
Katedra (ústav): Ústav částicové a jaderné fyziky
Vedoucí bakalářské práce: RNDr. Alice Valkárová, DrSc.
e-mail vedoucího: alice.valkarova@mff.cuni.cz

Abstrakt: V předložené práci je studována produkce Higgsova bosonu Standardního modelu v centrálních difrakčních procesech, přičemž se zaměřujeme na WW rozpadový mód. Hlavní část této práce spočívá v simulaci vzájemných interakcí protonů na LHC urychlovači v CERNu pro různé hmotnosti Higgsova bosonu užitím Monte Carlo modelu ExHuME. Získaná data byla následně zpracována a analyzována systémem ROOT určeným k analýze fyzikálních dat. Zjistili jsme, že ačkoli bude počet v této práci studovaného typu srážek malý, lze očekávat, že pro hmotnosti Higgsova bosonu nad 140 GeV bude detekovatelný.

Klíčová slova: difrakce, Higgsův boson, program ExHuMe

Chapter 1

Theoretical introduction

1.1 The Higgs' Mechanism in the Standard Model

At present, one of the key problems of particle physics is unraveling the mechanism that breaks the electroweak symetries and generates the masses of the fundamental particles - electroweak gauge bosons, leptons and quarks (see e.g. [1, 2]). There is wide range of scenarios extending from weak to strong breaking mechanisms. On one side it is the Standard Model and its supersymmetric extension involving light fundamental Higgs' fields, on the other side there are new strong interaction models without the fundamental Higgs' field. So it's clear that there is only one posibility how to resolve this problem: to make proper experiments.

The Higgs' mechanism [1, 3] is a cornerstone in the electroweak sector of the Standard Model. It was postulated by British physicist Peter Higgs in the 1960s and it assumed the existence of the scalar Higgs' field, which is non-zero in the ground state. Masses of the fundamental particles are then generated through the interaction (mediated by Higgs' bosons) with this field.

The Standard Model requires one complex Higgs' field doublet and predicts a single neutral Higgs' boson of unknown mass. After extensive searches at LEP (Large Electron-Positron Collider, CERN), a lower bound of 114.4 $\mathrm{GeV/c^2}$ has been established for the mass of the Standard Model Higgs' boson, at the 95% confidence level [4]. However, there is a strong belief that the Standard Model, in its minimal form with a single Higgs, cannot be the fundamental theory of particle interactions. Various extended models predict a large diversity of Higgs-like bosons with different masses, couplings and even CP-parities. The most elaborated extension of the Standard Model is

its supersymetric (SUSY) extension called Minimal Supersymmetric Standard Model (MSSM) (reviewed e.g. in [5]), that requires two Higgs' field doublets and predicts the existence of three neutral (h and H are CP-even, A is CP-odd) and two charged (H^+,H^-) Higgs' bosons. The lightest of the neutral ones, h, is predicted to have a mass less than about 140 GeV/c^2 and more than about 92 GeV/c^2. At tree level, two parameters are sufficient (besides the known parameters of the Standard Model fermion and gauge sectors) to fully describe the Higgs' sector. A convenient choice is the pseudoscalar Higgs' boson mass (m_A is chosen for CP-conserving scenarios and $m_{H^\pm}$ in CP-violating scenarios) and the ratio of the vacuum expectation values of the two Higgs' doublet fields, tanβ. At tree level, the pseudoscalar A does not couple to the gauge bosons and its couplings to down- (up-) type fermions are inversely proportional to tanβ.

Now I would like to introduce short overview about the Higgs' boson production at the LHC (Large Hadron Collider, CERN). It has emerged that Higgs' boson production in association with two jets could be a promising channel for Higgs' boson discovery and for the study of its properties. Interest has concentrated on vector-boson-fusion (VBF) [1], i.e. the weak process $qq \to qqH$ which is mediated by t channel exchange of a W or Z, with the Higgs' boson being radiated off this weak boson. The VBF production cross section measures the strength of the WWH and ZZH couplings, which, at tree level, require a vacuum expectation value for the scalar field. Hence the VBF channel is a sensitive probe of the Higgs' mechanism as the source of electroweak symmetry breaking.

Another significant source of Hjj events are second order real emission corrections to the gluon fusion process. Such corrections were first considered in Ref. [6, 7] in the large top mass limit and have subsequently been evaluated for arbitrary quark masses in the loops which induce the effective coupling of the Higgs' boson to gluons [8]. Some representative Feynman's graphs are shown in Figure 1.1.

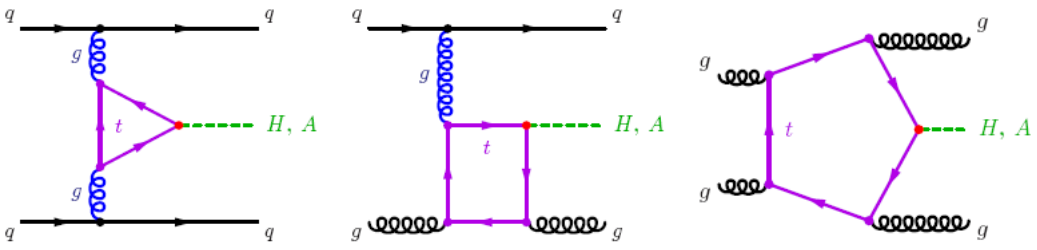

Figure 1.1: Feynman diagrams for $qq \to Hjj$; taken from [10].

1.2 Diffraction in particle physics?

In the next section basic concepts of the diffraction will be introduced. But firstly, the term "diffraction" should be clarified. From optics is known that light of wavelength λ impinging on a black disk of radius R_0 produces on a distant screen a diffraction pattern. It is characterized by a large forward peak for scattering angle $\theta = 0$ and a series of symmetric minima and maxima. The intensity I as a function of the scattering angle θ is given by

$$\frac{I(\theta)}{I(\theta = 0)} \simeq 1 - \frac{R^2}{4}(k\theta)^2, \tag{1.1}$$

where $k = 2\pi/\lambda$. So the diffraction relates to the size of the target and to the wavelength.

It was shown (for example [9]) that the differential cross section of proton-proton scattering is given by

$$\frac{\frac{d\sigma}{dt}(t)}{\frac{d\sigma}{dt}(t = 0)} \simeq e^{-b|t|} \simeq 1 - b(P\theta)^2, \tag{1.2}$$

where $|t| \simeq (P\theta)^2$ is the absolute value of the squared four-momentum transfer, P is the incident proton momentum and θ is the scattering angle. The t-slope b can be written as $b = R^2/4$, where once again R is related to the target size (or more precisely to the transverse distance between projectile and target). A dip followed by a secondary maximum has also been observed. So as we can see (by comparison of Eq. 1.1 and Eq. 1.2) that there is a remarkable resemblance between optic diffraction and proton-proton scattering. Therefore the term "diffraction" is used for elastic pp scattering. Similar t distributions have been observed for the other diffractive reactions (mentioned in the next section), leading to the use of the term diffraction for all such processes.

1.3 Diffraction - basic concepts

In hadron-hadron scattering a substantial fraction of the total cross section is due to diffractive reactions. There are three main types of these hadron-hadron diffractive processes (Fig. 1.2): elastic scattering, single dissociation and double dissociation. In the first one both hadrons emerge intact in the final state, whereas single or double diffractive dissociation corresponds to one or both of them being scattered into a low-mass state; the latter has the same quantum numbers as the initial hadron and may be a resonance or continuum state. The energy of the outgoing hadrons a, b or the states X, Y is approximately equal to that of the incoming beam particles, to within a few per cent. From Fig. 1.2 we can see, that there is a large gap in rapidity between the two groups of final-state particles (the absence of hadronic activity). This is unique and very useful advantage of these diffractive processes and it will be mentioned once more later.

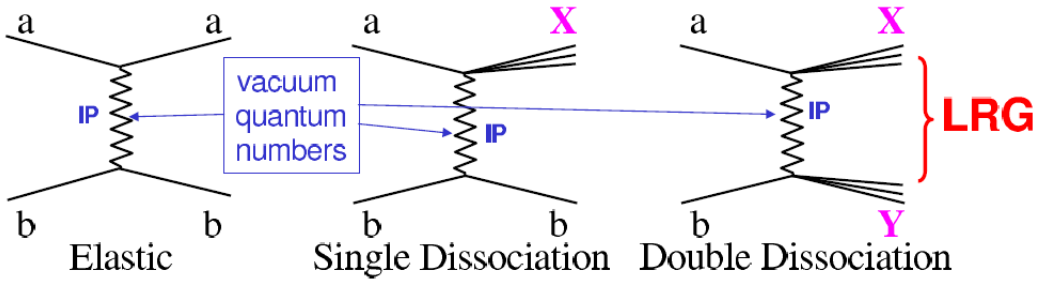

Figure 1.2: Types of diffractive processes in the collision of two hadrons. The zigzag lines denote the exchange of a Pomeron in the t-channel. There exist further graphs with multiple Pomeron exchange. Taken from [11].

Diffractive hadron-hadron scattering can be described within Regge theory (see e.g. [12]). In this framework, the exchange of particles in the t-channel is summed coherently to give the exchange of so-called "Regge trajectories". Diffraction is characterized by the exchange of a specific trajectory, the "Pomeron", which has the quantum numbers of the vacuum. Regge theory has spawned a successful phenomenology of soft hadron-hadron scattering at high energies. Developed in the 1960s, it predates the theory of the strong interactions, QCD, and is based on general concepts such as dispersion relations. Subsequently it was found that QCD perturbation theory in the high-energy limit can be organized following the general concepts of Regge theory; this framework is often referred to as BFKL after the authors of the seminal papers [13].

It is clear that a t-channel exchange leading to a large rapidity gap in the

final state must carry zero net color: if color were exchanged, the color field would lead to the production of further particles filling any would-be rapidity gap. In QCD, Pomeron exchange is described by the exchange of two interacting gluons with the vacuum quantum numbers.

The effort to understand diffraction in QCD has received a great boost from studies of diffractive events in ep collisions at HERA (see e.g. [14]). One of the essential results of these studies is that many aspects of diffraction are well understood in QCD when a hard scale is present, which allows one to use perturbative techniques and thus to formulate the dynamics in terms of quarks and gluons.

The production of the Higgs' boson in diffractive pp collisions is drawing more and more attention as a clean channel to study the properties of a light Higgs' boson or even discover it. The theoretical challenge is to adapt and apply the techniques for the QCD description of diffraction in ep collisions to the more complex case of pp scattering at the LHC.

1.4 Decay channels of the Higgs boson

Higgs' boson is the particle that decays, in very short time, into pairs of fermions or weak bosons. Once we assume a value for its mass, it is possible to compute the rates for Higgs' boson decay into these pairs of particles. Since we are not able to observe it directly (but only through its products) we have to choose the convenient decay channel. In Figure 1.3 there are branching fractions for decay modes that may hold promise for the detection of the Higgs' boson.

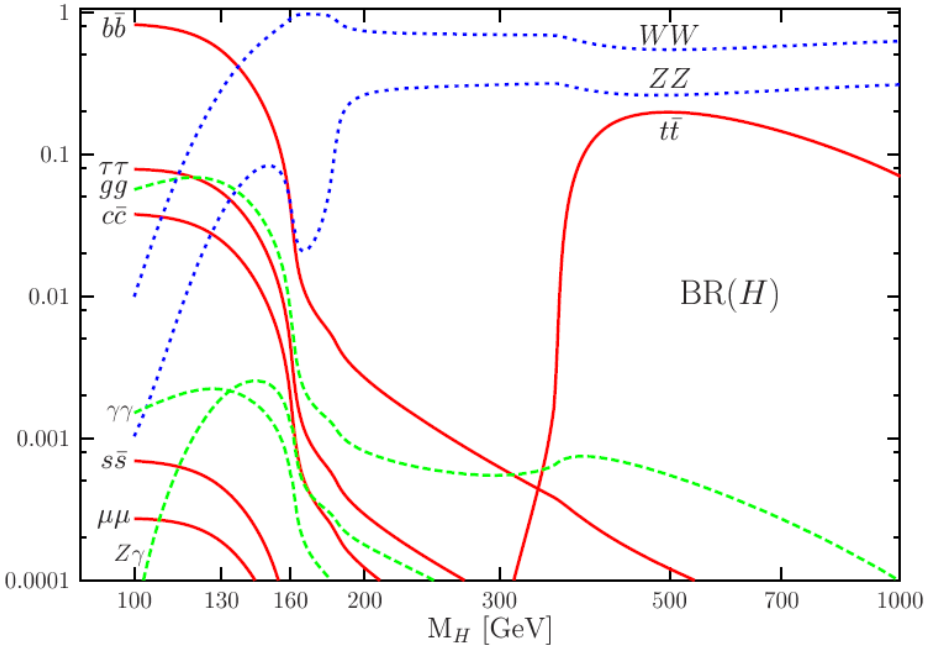

Figure 1.3: Branching fractions for the prominent decay modes of a light Higgs' boson; taken from [1].

As we can see from this figure there is a lot of decay channels of the light Higgs' boson. In sections 1.5 and especially 1.7 two most interestig of them($H \to b\bar{b}$, $H \to WW$) will be discussed because of their close relation to this bachelor thesis. Let me only say that the first one is dominant for masses below about 130 GeV and moreover it becomes extremely important in the so-called intense coupling regime[1] [16] of the MSSM. The latter is, in

[1]It is the case, when the masses of the two CP-even h, H and of the CP-odd A boson

the contrary, dominant for masses above about 130 GeV.

The huge QCD–jet backgrounds prevents from detecting the produced Higgs' boson (and any particle in general) in fully hadronic modes. When ignoring the light quark and gluon modes, the Higgs decays (see Fig. 1.3) mostly into $b\bar{b}$, $\tau\tau$, WW, ZZ and $\gamma\gamma$, $Z\gamma$ final states in the mass range below about 160 GeV and into WW, ZZ and $t\bar{t}$ final states above this mass value. In order to extract a signal in the entire Higgs' mass range, following requirements have to be met:

- In the decay modes WW, ZZ, at least one of the W/Z bosons has to be observed in its leptonic decays which have small branching ratios, $\mathrm{BR}(W \to l\nu) \simeq 20\%$ with $l = e, \mu$ and $\mathrm{BR}(Z \to l^+l^-) \simeq 6\%$. In the latter case the invisible neutrino decays, $\mathrm{BR}(Z \to \nu\nu) \simeq 18\%$, can also be sometimes used to increase the statistics. A very good detection of isolated high transverse momentum muons and electrons and an accurate calorimetry with hermetic coverage to measure the transverse energy of the missing neutrinos is thus required.

- A very high resolution on the photons is necessary to isolate the narrow $\gamma\gamma$ signal peak in the decay $H \to \gamma\gamma$ from the large continuum $\gamma\gamma$ background. Since the Higgs' boson width is small, a few MeV for $M_H \simeq 120$–140 GeV, the measured mass peak is entirely dominated by the experimental resolution. Furthermore, the very large number of high transverse momentum π^0 decaying into two photons, should be rejected efficiently.

- In the dominant Higgs' decay mode in the low mass range, $b\bar{b}$, excellent microvertex detectors are needed to identify the b–quark jets with a high efficiency and a high purity. τ–lepton identification is also important to detect the decays $H \to \tau^+\tau^-$ and the invariant mass of the final state should be reconstructed with a good resolution.

Beyond the Standard Model the properties of the neutral Higgs' bosons can differ drastically from SM expectations, so after the discovery of a Higgs' candidate the immediate task will be to establish its quantum numbers, to verify the Higgs' interpretation of the signal, and to make precision measurements of its properties. The separation and identification of different Higgs-like states will be especially challenging. In [15] was shown that the central exclusive diffractive processes (see next chapter) can play a crucial role in solving these problems.

(see chapter 1.1) are close to one another and the tan β is large.

1.5 Central exclusive diffractive processes

In the section 1.3 there is a short overview of diffractive processes in particle physics in general. Diffractive processes in proton collisions are those in which color singlet objects are exchanged between the high energy initial protons, which allow them to be diffracted. This can occur, for instance, when two gluons are exchanged in the t–channel (in this way Higgs production occurs) by the initial protons; this neutralizes the color and allow the two protons to remain intact and continue their way. Now let's have a look at a particular ones, the central exclusive diffractive processes (CEDP; see Figure 1.4a), that play a crucial role in the aim to discover the Higgs' boson and to determine its properties.

These processes (see for example [17, 18]) are of the form

$$pp \to p \oplus \phi \oplus p, \tag{1.3}$$

where the sign $\oplus$ denotes the absence of hadronic activity (so-called 'gap') between the outgoing protons and the decay products of the central system ϕ. These processes have unique advantages as compared to the traditional non-diffractive approaches. Firstly, if the outgoing protons remain intact and scatter through small angles, then, to a very good approximation, the central system ϕ is produced in the $J_z = 0$, C and P even state. An absolute determination of the quantum numbers of any resonance is possible by measurements of the correlations between outgoing protons momenta. Secondly, if the forward protons are tagged, then, contrary to a conventional inelastic production, the mass of the produced central system ϕ can be measured to high accuracy by the missing mass method (from a measurement of momentum components of the outgoing protons).

All models for hard diffractive production in central region involve a mixture of perturbative and non-perturbative QCD physics, which is not well understood yet. In Figure 1.4 there is illustration of three processes for double-diffractive Higgs production in hadronic collisions.

In the first case, Figure 1.4a, the produced Higgs is separated from the outgoing protons by large rapidity gaps. To be able to determine Higgs' mass the outgoing protons must be tagged (more about tagging in the next chapter). The mass can be measured in two independent ways: by the missing mass method or by reconstructing the $H \to b\bar{b}$ decays mass peak. In the $b\bar{b}$ decay mode the potentially copious b-jet background is suppressed by a combination of a spin selection rule ($J_z = 0$) and the mass resolution from the tagging detectors. Although this channel is attractive (it is dominant for light Higgs) it is complicated to realize it. One reason is the mass resolution of

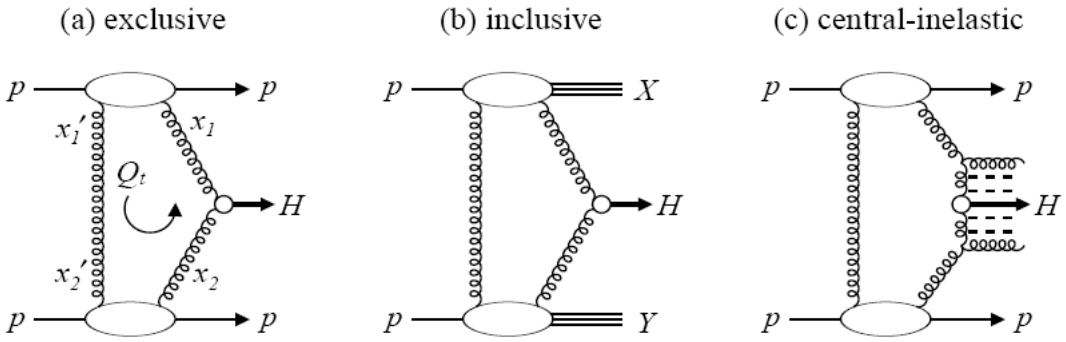

Figure 1.4: Double-diffractive Higgs production in pp collisions.; taken from [19].

the proton taggers, that is used to suppress the remaining b-jet background[2].

In the Figure 1.4b there is depicted the inclusive process for double-diffractive Higgs production. The advantage is much larger cross section, however there is no spin selection rule to suppress the $b\bar{b}$ background, so the signal-to-background ratio is unfavourable.

The last depicted process, 1.4c, is central inelastic production ($pp \rightarrow p + (HX) + p$). There is additional radiation accompanying the Higgs in the central region, which is separated from the outgoing protons by rapidity gaps. It seems that this mechanism has no special advantages for Higgs detection.

[2]The remaining b-jet background is a continuum beneath the Higgs mass peak, so poor resolution allows more background events into the mass window around the peak.

1.6 Large Hadron Collider and its detectors

The Large Hadron Collider (LHC) is located at CERN, near Geneva (Switzerland). Currently it is under construction and it is scheduled to begin operation in November 2007, at reduced luminosities and energies first. It is designed to collide beams of protons and Pb ions, protons at centre-of-mass energy 14 TeV. However, the beams aren't continuous. The protons will be collected in 2808 bunches, each of them about 1.15 x 10^{11} particles, so it makes energy about 362 MJ per beam. The bunches will be smashing together every 25 ns (frequency 40 MHz). At the high luminosity mode ($10^{34} cm^{-2} s^{-1}$) it is expected to see on average 23 overlapping hadronic interactions per bunch crossing.

One of the key characteristics of colliders is their luminosity. It is a factor of proportionality between number of events generated per second N_{events} and cross section σ_{events}

$$N_{events} = L\sigma_{events}. \tag{1.4}$$

There are six detectors that will study what happens in the interaction points. Two of them are large, ATLAS (A Toroidal LHC ApparatuS) and CMS (Compact Muon Solenoid), aiming at a peak luminosity of $10^{34} cm^{-2} s^{-1}$ (high luminosity experiments) in proton operation. The other ones are smaller and more specialized. It is LHCb (LHC beauty) aiming at a peak luminosity of $10^{32} cm^{-2} s^{-1}$ and TOTEM (for detection of protons from elastic scattering at small angles; it shares intersection point with CMS) aiming at $L = 10^{29} cm^{-2} s^{-1}$. One experiment at LHC is dedicated to ion experiments: ALICE (A Large Ion Collider Experiment), aiming at $L = 10^{27} cm^{-2} s^{-1}$ for Pb-Pb operation. And finally there is LHCf (LHC forward), that shares interaction point (IP) with ATLAS.

TOTEM experiment is designed to measure the total and elastic pp cross sections and the diffraction dissociation. It will use two telescopes to detect inelastic events and three so called Roman Pots (RP), that are designed to measure protons scattered under very small angles (defined with respect to the beam axis). The RP detectors in general allow us to measure protons' momenta and so they can be used to determine the mass of the centrally produced object, in this case Higgs' boson.

As mentioned in previous section, CEDP are characteristic by the presence of rapidity gaps and nondissociated protons. However, at the highest luminosities it isn't possible to observe any rapidity gaps due to overlapping events. That is one of the reasons why RP detectors are needed. They will be installed in the ATLAS (detecting decay products of the Higgs) [20] as well and so it will be possible to reconstruct the kinematics of these events

thanks to their good resolution.

There are several location around the ATLAS interaction point at which it is possible to install forward proton tagging detectors. It is 220 m region, where is proposed the installation of two sets of RP (at 216 m and 224 m) [20] and the 420 m region[3], where are detectors sensitive to lower masses (since they are located further away from the interaction point). The acceptance goes down to 100 GeV and decreases rapidly as a function of mass for the 420 m detectors whereas the acceptance of the 220 m pots starts at about 140 GeV. If both protons are detected at 420 m from IP, the missing mass resolution for a 140 GeV central system will be $\sigma \sim 1\%$. If one proton is detected at 220 m and the other at 420 m, the resolution will be approximately 6%. The detectors at 220 m alone can accept only central systems with masses larger than 200 GeV/c^2.

[3]There can't be, however, installed roman pots since it is in the cryogenic region of the LHC. The technology for both projects is different.

1.7 The WW decay channel

The aim of this section is to choose a convenient decay channel of the Higgs' boson that will allow us, with respect to technical characteristics of detectors, to decide whether we are observing decay products of Higgs or not. As the title of this section indicates, the channel of our interest will be the WW.

As mentioned in section 1.4, there exist many decay channels, see Fig. 1.3, among them the most interesting ones are $b\bar{b}$ and WW. As was also mentioned, the first one is attractive, because it allows direct access to the dominant decay mode of the light Higgs. However, there are two unpleasantnesses in this process. One of them was described in section 1.5: there is b-jet background that is suppressed by the mass resolution of taggers, so any degradation in the expected resolution will adversely affect the signal to background ratio. With this problem relates the acceptance-resolution compromise. Lets say we will detect the 120 GeV/c^2 Higgs. In this case we can choose from two detecting modes: the combination of 220 and 420 m detectors or the 420 m alone. While the first one gives reasonable acceptance and a rather moderate resolution, the latter offers a rather low acceptance and the excellent resolution leading to the efficient background suppression. Another problem is in positions of roman pots: due to the latency requirements, singals from detectors behind 215 m would arrive too late to the central trigger to be included in its first level [21].

The WW mode, however, does not suffer from either of the above problems. Suppression of the dominant backgrounds does not rely primarily on the mass resolution of the RPs and certainly in the leptonic and semi-leptonic decay channels level 1 triggering is not a problem [21]. From an experimental point of view there are three main categories of events with two W bosons in final state. The first one is when at least one W boson decays in either the e or μ channel. These events will usually pass the level 1 trigger thresholds due to the high transverse momentum of the final state lepton. If any of the W bosons does not decay in the e or μ channel there still exists possibility to pass the level 1 trigger thresholds: it is when W decays in the τ channel (τ decaying leptonically). The last main category of events is the 4-jet decay mode. It occurs approximately half the time, but it is unlikely that it will pass the level 1 triggers without information from the RPs.

In a Table 1.1 there are shown cross sections and number of events for the semi-leptonic and fully-leptonic decay channel [21]. There are used the ATLAS trigger thresholds and contrary to the original table numbers of events per the luminosity of 30 fb^{-1} are recounted to events per 100 fb^{-1}, which is the expected integrated luminosity of the LHC per year in high luminosity

mode.

Standard trigger thresholds for ATLAS are:

- Single lepton trigger:
  an electron with p_T>25 GeV or a muon with p_T>20 GeV, all within $|\eta|$ <2.5

- Fully-leptonic trigger:
  $2e(p_T^e$>15 GeV) or $2e(p_{T,max}^e$>25 GeV)
  or $2\mu(p_T^\mu$>10 GeV) or $2\mu(p_{T,max}^\mu$>20 GeV)
  or $e\mu(p_T^e$>15 GeV and p_T^μ>10 GeV)
  or $e\mu(p_T^e$>25 GeV or p_T^μ>20 GeV),
  all within $|\eta|$ <2.5

Selection cuts	**Higgs' mass [GeV]**	**Efficiency**	σ **[fb]**	**Events / 100 fb^{-1}**
Generated $H \to WW$	120	100 %	0.403	40.3
	140	100 %	0.933	93.3
	160	100 %	1.164	116.4
Acceptance of proton taggers (420 m + 220 m)	120	61 %	0.246	24.6
	140	67 %	0.625	62.5
	160	71 %	0.826	82.6
Single lepton trigger	120	8.7 %	0.035	3.5
	140	12.8 %	0.119	11.9
	160	16.6 %	0.194	19.4
2 or more jets within $\|\eta\|$ <2.5	120	7.0 %	0.028	2.7
	140	10.2 %	0.096	9.7
	160	13.6 %	0.158	15.7
Mass window around hadronically decaying W 70 GeV $<M_W<$90 GeV	120	0.54 %	0.002	0.3
	140	2.0 %	0.019	2.0
	160	7.2 %	0.084	8.3
p_T(protons)>100 MeV	120	-	-	-
	140	-	-	-
	160	6.6 %	0.077	7.7
p_T(protons)>200 MeV	120	-	-	-
	140	-	-	-
	160	5.2 %	0.061	6.1
Fully-leptonic triggers	120	2.3 %	0.009	0.9
	140	3.1 %	0.029	2.9
	160	3.3 %	0.038	3.8
p_T(protons)>100 MeV	120	-	-	-
	140	-	-	-
	160	3.1 %	0.036	3.6
p_T(protons)>200 MeV	120	-	-	-
	140	-	-	-
	160	2.4 %	0.028	2.8

Table 1.1: Standard ATLAS lepton trigger thresholds (see previous page) for semi-leptonic (middle part) and fully-leptonic (botoom part) events; taken from [21].

Chapter 2

Simulation programs

2.1 Monte Carlo generators for diffraction

Monte Carlo simulation methods are, in general, a mathematical tools used to solve problems (numerically) that are too complicated to be solved analytically, for example integral calculus. In contrast to other simulation methods, this ones are stochastic (nondeterministic) - their nature is in generating suitable (pseudo-)random numbers. Monte Carlo method is especially effective in solving problems with a large number of degrees of freedom. Its efficiency relative to other numerical methods increases with increasing dimension of the problem.

In nuclear and particle physics (or, more accurately, in processes involving quantum mechanics) a concept of randomness plays a key role in a behaviour of physical systems and Monte Carlo techniques allow us to simulate this randomness. The essential part of event generator is then a random number generator. In practice, however, is used pseudorandom number generator approximating properties of random numbers.

In section 1.5 there are defined and described central exclusive diffractive processes. At present, there are three Monte Carlo generators that can be used to simulate them: DPEMC [22], EDDE [23] and ExHuME [24]. These models of central exclusive production are either perturbative (ExHuME) or non-perturbative (DPEMC, EDDE).

ExHuME is the Monte Carlo program based on calculation of V. A. Khoze et al [25], known as Durham Model. This approximation includes a Sudakov factor to suppress radiation into the rapidity gaps and a survival factor, S^2, to ensure that there are no additional interactions between the proton lines. The current default value is 0.03 at the LHC.

In contrast, DPEMC and EDDE are non-perturbative models which use the Regge theory (pomeron exchange from each of the proton lines). DPEMC is based on Bialas-Landshoff approach [26] and it also sets the value of S^2 to 0.03 at the LHC. EDDE uses an improved Regge-eikonal approach [27] and includes a Sudakov suppression factor, but not explicit survival factor.

In each of these Monte Carlos are similar available processes (e.g. Higgs' boson production with all subsequent decays). Di-jet production is also included in all three generators. However, none of Monte Carlos includes next-to-leading order three jet process, which could be very important background to the central exclusive $H \to b\bar{b}$ channel. All three generators give similar predictions for the cross section, but the physics potential decreases for models that include Sudakov suppression, which will limit Higgs' boson searches.

2.2 ExHuME generator

In the previous section there are mentioned three Monte Carlo simulation programs used for central exclusive processes. In this section we will focus to one of them, Exclusive Hadronic Monte Carlo Event generator (ExHuME).

In Figure 2.1 there is shown the leading order diagram for central exclusive production, which ExHuME factorises as indicated by the dashed line. In this initial version of ExHuME there are provided $gg \to H$, $gg \to Q\bar{Q}$ (Q is a massive quark) and $gg \to gg$ sub-processes.

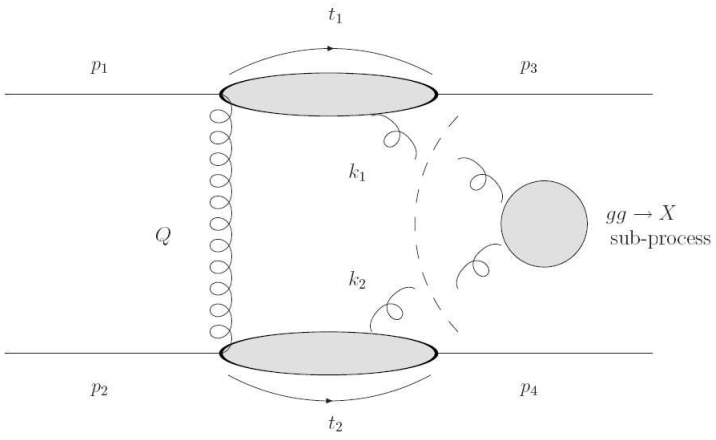

Figure 2.1: The leading order diagram for CEDP of system X; taken from [24].

ExHuME is a C++ program designed to use Pythia [28] for the purposes of hadronisation. Pythia is a program for generation of high-energy events, i.e. for the collisions between elementary particles, in particular interactions in e^+e^-, pp and ep colliders. This event generator contains a wide range of reactions not only within the Standard Model, but beyond it as well (although the physics of processes where strong interactions are involved is not always understood well enough to give an exact description).

ExHuME is written in a C++ object oriented programming language. It includes two main classes: 'CrossSection' class is for calculation of differential luminosity, gluon fusion sub-process and kinematics of outgoing particles and allow us for example to set the decay mode of the Higgs; 'Event' class is used for generation of the events and it is able to calculate the total cross section and efficiency of event generation. For comprehensive description of its structure and using see [24].

2.3 Simulations and their analysis

The main part of this thesis is to simulate and analyze events of the form $p + p \rightarrow H \rightarrow WW$. To performe this task the ExHuME program is used first and then the gained data processed by the use of a data analysis system ROOT [29].

The ExHuME program in its basic form generates and writes complete events either directly on screen or the output can be redirected to a file. For purposes of generation hundreds of thousands events the output files would be of a big size and so their subsequent processing would be demanding. Since there is no need to know complete events but only leptons originating directly from decays of W bosons, I've decided to write only them. In the case that the lepton is tauon, only processes $\tau \rightarrow e/\mu$ (directly) are taken and such electrons and muons, not original tauon, are written.

The output of the ExHuME is of the form Pythia's event record. It assigns to every particle in the event a set of parametrs such as a particle identification code (KF), components of its momenta, energy or line numbers of parent particle and first and last daughter. It turned out that it would be advantageous to proceed subsequently: first to find out whether at least one W decays in leptonic channel. If it does and there is an unstable lepton, all stable electrons and muons (and their antiparticles) in the event are found. Their parents and parents of their parents and so on up to direct decay products of Ws are checked and if the last one agrees with the unstable electron or muon, the stable one is written to the output file. The same way is used to identify the e/μ from the process $\tau \rightarrow e/\mu$.

Previous paragraph describes briefly an adjustment of the ExHuME for our purposes. The other step is to process gained data by the ROOT system. I have written a script that reads the output file of the adjusted ExHuME and for every particle computes pseudorapidity and transverse momentum which are used to fill histograms. Beside this function the program evaluates numbers of electrons and muons that are able to pass the ATLAS triggers and so allow us to determine efficiencies of such triggers.

Chapter 3

Results

In the previous chapter there are decribed programs, that were used to simulate collisions of protons of the overall centre-of-mass energy 14 TeV at the LHC. In this chapter, results of such simulations will be introduced.

There are two main steps in gaining data. Firstly, the adjusted ExHuME (see section 2.3) of version 1.3.2 interfaced to Pythia (of version 6.408) event generator is used to simulate 100 000 events of our interest ($p+p \rightarrow H \rightarrow WW$) for various Higgs' masses. Our intention is to study events where at least one W decays in the leptonic channel (in the case of tauon, only events with its subsequent decay to electron or muon - or their antiparticles - are taken). Secondly, the output file gained in the previous step is processed (pseudorapidity and transverse momentum for each lepton are calculated) and by the use of a data analysis system ROOT [29] fitting histograms are created.

There are three possiblities how W bosons, originating from Higgs, can decay:

- 4-jet decay mode: $WW \rightarrow jjjj$
- Semi-leptonic decay channel: $WW \rightarrow l\nu jj$
- Fully-leptonic decay channel: $WW \rightarrow l\nu l\nu$

($l = e, \mu, \tau$, $\tau \rightarrow e/\mu$; $j =$ quarks causing jets)

According to my findings (ExHuME simulations), the ratio among these processes is almost constant for various Higgs' masses. The 4-jet decay mode occures in about 57 %, semi-leptonic and fully-leptonic channel in about 37 % and 6 % (for exact numbers for $m_H = 160$ GeV see Tab. 3.1). Although the 4-jet mode makes a slight majority, it shouldn't pass the level 1 trigger of ATLAS. However, according to [21] if the proton tagging detectors at 220m are included in the level 1 trigger, such events could be taken and so

increase the trigger efficiency.

In Fig. 3.1 there is depicted a transverse momentum distribution of events where at least one W decays in leptonic channel for Higgs' mass 160 GeV. A dashed line denotes a distribution of electrons and muons (and their antiparticles) originating directly from Ws, solid line denotes additional electrons and muons of τ decay. We can see that leptons from tauons have softer spectrum, most of them is to about 22 GeV. The percentage of tauons in semi- or fully-leptonic channel for Higgs' mass 160 GeV (for other masses it is very similar) is shown in Tab. 3.1.

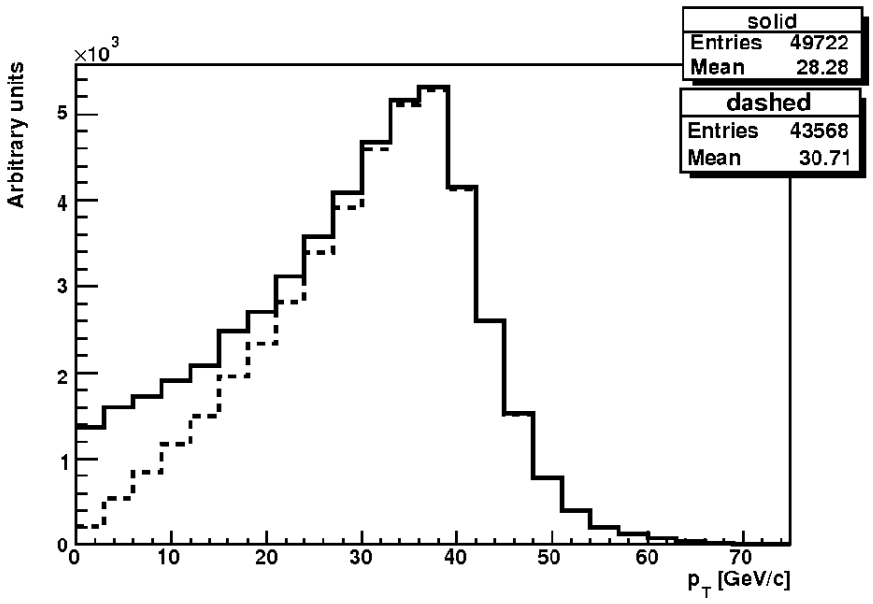

Figure 3.1: Transverse momentum distribution of electrons and muons (dashed line) and all electrons and muons including $\tau \rightarrow e/\mu$ (solid line). Semi- and fully-leptonic channels added together, Higgs' mass 160 GeV.

Another interesting histograms are pseudorapidity distributions. In Fig. 3.2 there is a distribution of pseudorapidity for Higgs' mass 160 GeV for at least one W decaying in leptonic channel (including tauons $\tau \rightarrow e/\mu$). The mean value is, as expected, very close to zero. The shape of these histograms for other Higgs' masses is very similar.

In Fig. 3.3 there are histograms of transverse momentum for six different masses of the Higgs' boson (in the range from 160 to 120 GeV) for at least one W decaying into leptonic state. We can notice interesting phenomenon: with decreasing Higgs' mass a width of this distribution is increasing and its

Process	Total number	Percentage
$WW \to l\nu jj$	37514	37.5 %
$WW \to \tau\nu jj$	4639	4.6 %
$WW \to l\nu l\nu$	6104	6.1 %
$WW \to \tau\nu ll$	1331	1.3 %
$WW \to \tau\nu\tau\nu$	92	0.09 %

Table 3.1: Representation of particular processes for Higgs' mass 160 GeV, total number of generated events is 100 000; $l = e, \mu$.

maximum is slowly moving to lower transverse momenta. When the mass reaches the value of 120 GeV, we can see two clear maxima. It indicates that there are in fact two composing distributions, one of them is greater than the other one for high Higgs' masses, for low Higgs' masses the ratio turns around.

Better way to observe this phenomenon is for fully-leptonic channel which allow us to distinguish leptons originating from W bosons with respect to their transverse momenta. The Fig. 3.4 contains histograms for 160, 140 and 120 GeV Higgs' masses. The $W \to \tau \to e/\mu$ decay isn't included because of the softer spectrum of such leptons (as discussed above, Fig. 3.1). We can see that there are two composing distributions for each m_H and with decreasing mass the lower p_T ones are more and more focused around their mean value that moves with decreasing mass to lower momenta: the values for m_H = 160, 140, 120 GeV/c are $< p_T >_{min}$ = 23.9, 18.6, 13.8 GeV/c, $< p_T >_{max}$=37.2, 34.7, 31.8 GeV/c. These differeces are caused by different properties of each W boson (in process $H \to WW$) and so we can observe the same shape of distribution for semi-leptonic channel as in Fig. 3.4 (a), (c), (e) for fully-leptonic mode.

In Table 3.2 there are counted cross sections and number of events per 100 $\mathrm{fb}^{-1}\mathrm{y}^{-1}$ (expected LHC luminosity) for both semi- and fully-leptonic channels. In the line 'Generated' there are cross sections that were gained from ExHuME simulation program, in the rest of the table they are recounted with respect to the efficiency. The efficiency of proton taggers is taken from [21], for the semi- and fully-leptonic triggers it is calculated from analysis of generated events. Standard trigger thresholds for ATLAS are in section 1.7.

By the comparison of Tab. 1.1 and Tab. 3.2 we see that the results are similar. Cross sections for $H \to WW$ process are smaller for all Higgs' masses than the ones from Tab. 1.1. It can be caused by the different versions of ExHuME program (our version 1.3.2, in [21] it is 1.3) and Pythia

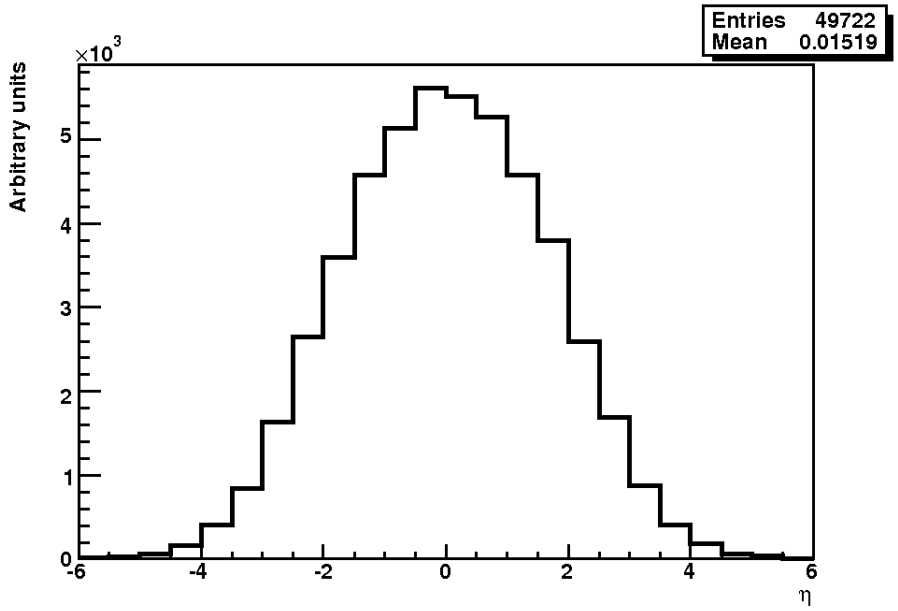

Figure 3.2: Pseudorapidity distribution for $m_H = 160$ GeV, semi- and fully-leptonic channels together.

event generator (our version 6.408, in [21] 6.205). Furthermore we see that our efficiencies for single lepton trigger are slightly higher, the other cuts (p_T protons above 100 MeV and 200 MeV) can't be compared because in Tab. 1.1 there are applied additional cuts that were not considered in this thesis. By the comparison of fully-leptonic triggers (this time we can compare all cuts) we see that efficiencies are slightly higher again. These small differencies between results of work [21] and ours can be explained by the use of different versions of ExHuME simulation program.

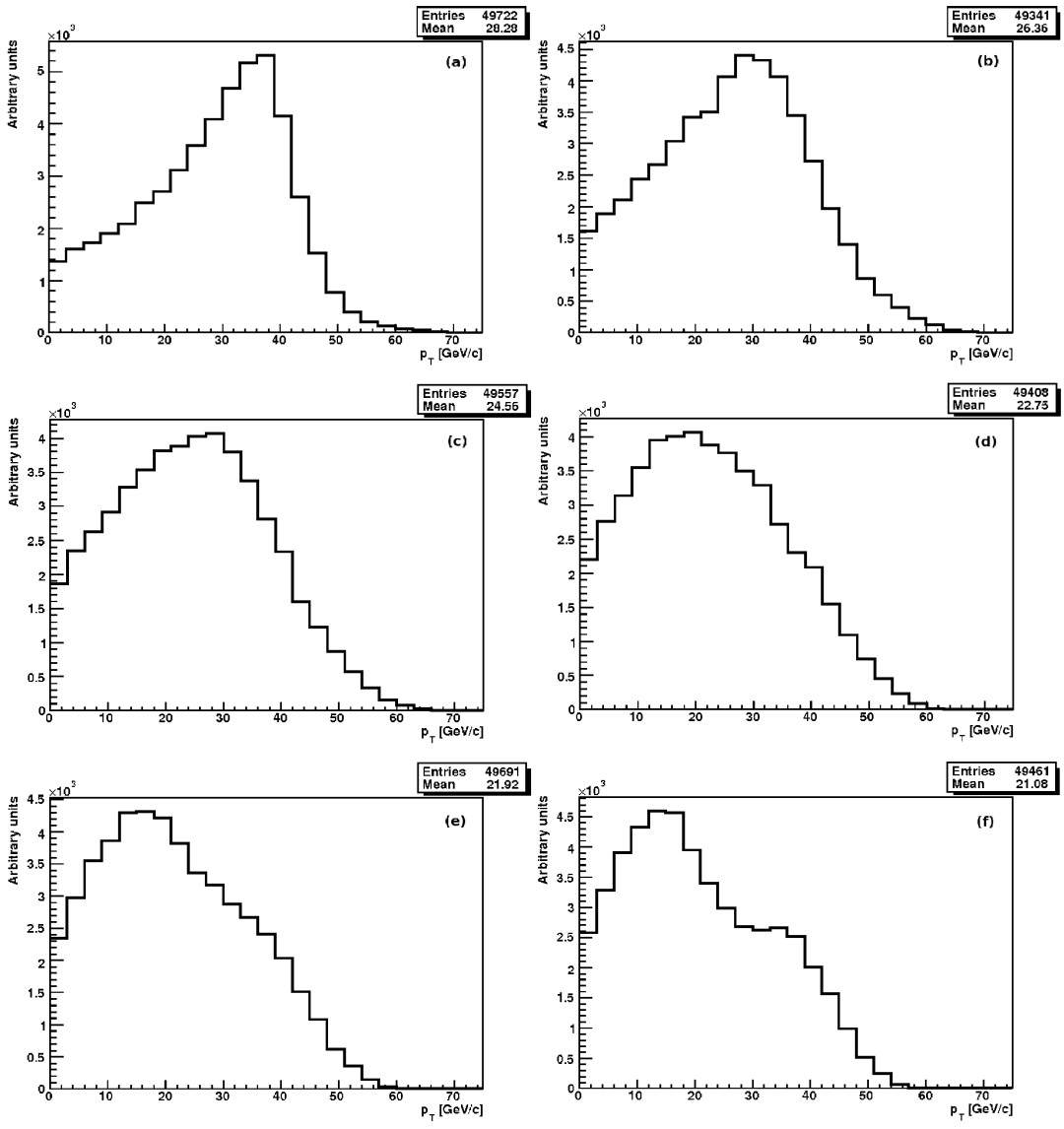

Figure 3.3: Transverse momentum distributions for various masses of the Higgs' boson: (a) 160 GeV, (b) 150 GeV, (c) 140 GeV, (d) 130 GeV, (e) 125 GeV, (f) 120 GeV

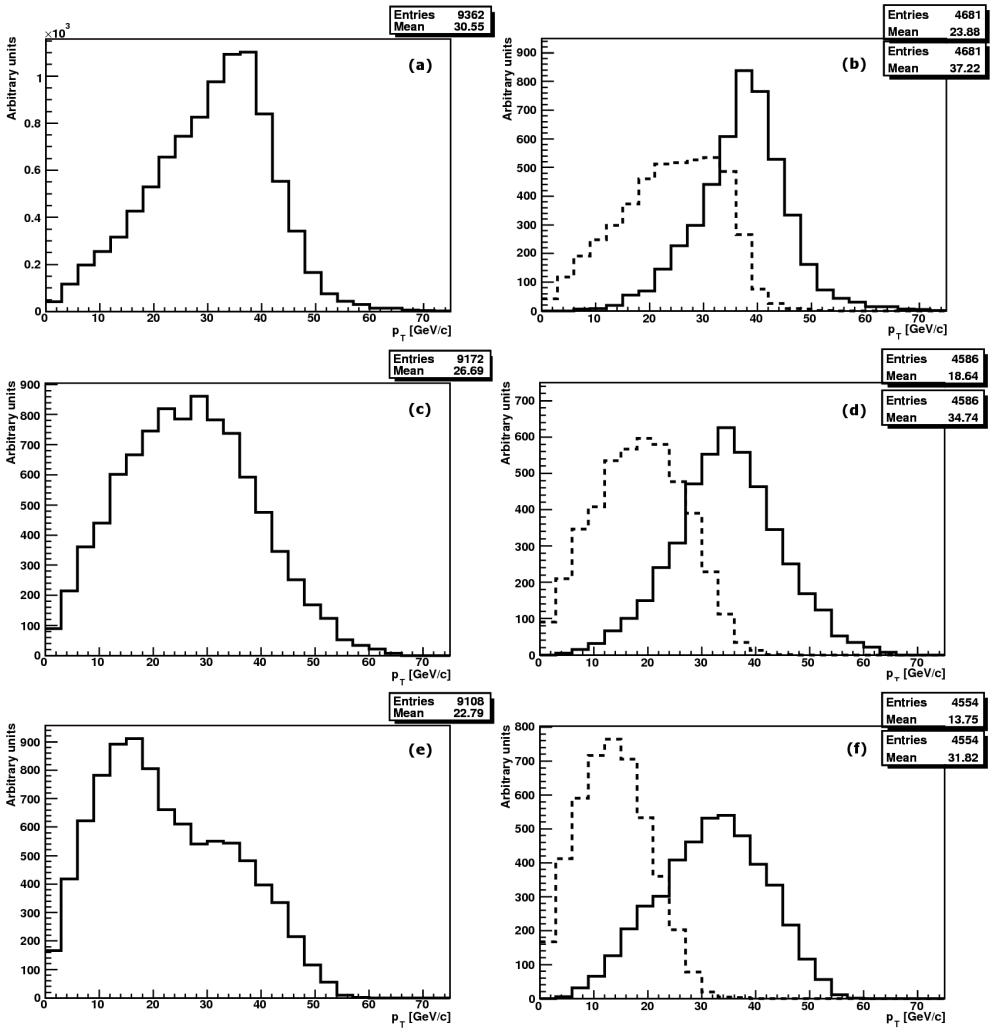

Figure 3.4: Transverse momentum distributions for fully-leptonic channel (without tauons) of Higgs' mass: (a)&(b) 160 GeV, (c)&(d) 140 GeV, (e)&(f) 120 GeV. In each histogram (b), (d), (f) is a distribution of leptons with higher (solid line) and lower (dashed line) p_T. The sum of these two distributions gives histograms on the left side, (a), (c) and (e).

Selection cuts	**Higgs mass [GeV]**	**Efficiency**	σ **[fb]**	**Events / 100 fb^{-1}**
Generated	120	100 %	0.370	37.0
	140	100 %	0.855	85.5
	160	100 %	1.062	106.2
Acceptance of proton taggers (420 m + 220 m)	120	61 %	0.226	22.6
	140	67 %	0.573	57.3
	160	71 %	0.754	75.4
Single lepton trigger	120	9.2 %	0.034	3.4
	140	13.2 %	0.113	11.3
	160	17.7 %	0.188	18.8
p_T(protons)>100 MeV	120	8.5 %	0.031	3.1
	140	12.2 %	0.104	10.4
	160	16.4 %	0.174	17.4
p_T(protons)>200 MeV	120	6.7 %	0.025	2.5
	140	9.6 %	0.082	8.2
	160	12.9 %	0.137	13.7
Fully-leptonic triggers	120	2.8 %	0.010	1.0
	140	3.4 %	0.029	2.9
	160	3.8 %	0.040	4.0
p_T(protons)>100 MeV	120	2.5 %	0.009	0.9
	140	3.1 %	0.027	2.7
	160	3.5 %	0.037	3.7
p_T(protons)>200 MeV	120	2.0 %	0.007	0.7
	140	2.4 %	0.021	2.1
	160	2.8 %	0.030	3.0

Table 3.2: Standard ATLAS lepton trigger thresholds for semi-leptonic (middle part) and fully-leptonic (botoom part) events. Acceptances of proton taggers are taken from [21].

Chapter 4

Conclusion

In the first chapter there is a basic summary of theoretical pieces of knowledge about the Standard Model Higgs' boson and central exclusive diffractive processes. The main part of this thesis is, however, in simulations of proton collisions at the LHC collider at CERN with centre-of-mass energy 14 TeV for different Higgs' boson masses (120, 140 and 160 GeV). These simulations were performed by the use of the ExHuME Monte Carlo program and subsequently processed and analyzed by ROOT data analysing system. Results of this analysis are introduced in Chapter 3.

In the Table 3.2 there are calculated cross sections and numbers of events per 100 $\mathrm{fb}^{-1}\mathrm{y}^{-1}$ (expected LHC luminosity). We have shown that these data are in accordance with previous findings [21]. For 220 m and 420 m proton tagging detectors at ATLAS and for standard ATLAS trigger thresholds it is possible to expect that Standard Model Higgs' boson will be detectable for Higgs' masses above 140 GeV. However, the number of such events per year will be very small (we can expect around 5 or 6 of them) and so the suppresion of a background will play a key role. The most dangerous background is in the semi-leptonic channel for Higgs' masses below 160 GeV. However, it is expected that it could be suppressed by carefully chosen cuts.

Bibliography

[1] Abdelhak Djouadi, The Anatomy of electro-weak symmetry breaking. I: The Higgs boson in the standard model, arXiv:hep-ph/0503172

[2] S. Heinemeyer *et al.*, Toward high precision higgs-boson measurements at the international linear e^+e^- collider, arXiv:hep-ph/0511332

[3] P.W. Higgs, Phys. Lett. 12 (1964) 132; Phys. Rev. Lett. 13 (1964) 508; Phys. Rev. 145 (1966) 1156;

[4] ALEPH, DELPHI, L3 and OPAL Collaborations, The LEP Working Group for Higgs Boson Searches, Phys. Lett. B565 (2003) 61, hep-ex/0306033

[5] Abdelhak Djouadi, The Anatomy of electro-weak symmetry breaking. II: The Higgs bosons in the minimal supersymmetric model, arXiv:hep-ph/0503173

[6] R. P. Kauffman, S. V. Desai, D. Risal, Production of a Higgs boson plus two jets in hadronic collisions, arXiv:hep-ph/9610541

[7] R. P. Kauffman, S. V. Desai, Production of a Higgs pseudoscalar plus two jets in hadronic collisions, arXiv:hep-ph/9808286

[8] V. Del Duca, W. Kilgore, C. Oleari, C. Schmidt and D. Zeppenfeld, Higgs + 2 jets via gluon fusion, arXiv:hep-ph/0105129; Gluon fusion contributions to H + 2 jet production, arXiv:hep-ph/0108030

[9] K. Goulianos, Phys. Rept. 101 (1983) 169

[10] G. Klämke and D. Zeppenfeld, arXiv:hep-ph/0703202

[11] M. Arneodo, M. Diehl, Higgs plus two jet production via gluon fusion as a signal at the CERN LHC, arXiv:hep-ph/0511047

[12] P. D. B. Collins, An Introduction to Regge Theory and High-Energy Physics, Cambridge University Press, Cambridge, 1977.

[13] E. A. Kuraev, L. N. Lipatov and V. S. Fadin, Sov. Phys. JETP 44 (1976) 443; ibid. 45 (1977) 199;
I. I. Balitsky and L. N. Lipatov, Sov. J. Nucl. Phys. 28 (1978) 822.

[14] M. Wüsthoff and A. D. Martin, J. Phys. G 25 (1999) R309 arXiv:hep-ph/9909362;
J. R. Forshaw and D. A. Ross, Quantum chromodynamics and the pomeron, Cambridge Lect. Notes Phys. 9 (1997) 1;

[15] A.B. Kaidalov, V.A. Khoze, A.D. Martin and M.G. Ryskin, Central exclusive diffractive production as a spin-parity analyser: From Hadrons to Higgs, arXiv:hep-ph/0307064

[16] E. Boos, A. Djouadi and A. Nikitenko, Detection of the neutral MSSM Higgs bosons in the intense coupling regime at the LHC, arXiv:hep-ph/0307079

[17] A. De Roeck, V. A. Khoze, A. D. Martin, R. Orava and M. G. Ryskin, Ways to detect a light Higgs boson at the LHC, arXiv:hep-ph/0207042

[18] V. A. Khoze, A. B. Kaidalov, A. D.Martin, M. G. Ryskin and W. J. Stirling, Diffractive processes as a tool for searching for new physics, arXiv:hep-ph/0507040

[19] V. A. Khoze, A. D Martin and M. G. Ryskin, Diffractive Higgs production: Myths and reality, arXiv:hep-ph/0207313

[20] M. Albrow et al., Prospects for diffractive and forward physics at the LHC, CERN-LHCC-2006-039, CERN-LHCC-G-124, CERN-CMS-NOTE-2007-002, Dec 2006

[21] B. E. Cox, A. De Roeck, V. A. Khoze, T. Pierzchala, M. G. Ryskin, I. Nasteva, W. J. Stirling and M. Tasevsky, Detecting the standard model Higgs boson in the WW decay channel using forward proton tagging at the LHC, arXiv:hep-ph/0505240

[22] E. Boonekamp, T. Kúcs, DPEMC: A Monte-Carlo for Double Diffraction, arXiv:hep-ph/0312273

[23] V. A. Petrov, R. A. Ryutin, A. E. Sobol, EDDE Monte Carlo event generator, arXiv:hep-ph/0409180.

[24] J. Monk and A. Pilkington, ExHuME: A Monte Carlo Event Generator for Exclusive Diffraction, arXiv:hep-ph/0502077

[25] V. A. Khozehe, A. D Martin and M. G. Ryskin, Prospects for new physics observations in diffractive processes at the LHC and Tevatron, arXiv:hep-ph/0111078

[26] A. Bialas and P. V. Landshoff, Phys. Lett. B B256, 540 (1991)

[27] V. A. Petrov and R. Ryutin, Eur. Phys. Journ C36, 509 (2004)

[28] T. Sjöstrand, S. Mrenna and P. Skands, JHEP05 (2006) 026, arXiv:hep-ph/0603175

[29] ROOT User Guide, *http://root.cern.ch/root/doc/RootDoc.html*